Real-Time LIDAR Imaging by Solid-State Single Chip Beam Scanner.

Jisan Lee, Kyunghyun Son, Changbum Lee, Inoh Hwang, Bongyong Jang, Eun Kyung Lee, Dongshik Shim, Hyunil Byun, Changgyun Shin, Otsuka Tatsuhiro, YongChul Cho, Kyoungho Ha, and Hyuck Choo[1]
[1]**Advanced Sensor Lab, Samsung Advanced Institute of Technology, Samsung Electronics, Korea**

Abstract

We present a real-time light detection and ranging (LIDAR) imaging by developing a single-chip solid-state beam scanner. The beam scanner is integrated with a fully functional 32-channel optical phased array, 36 optical amplifiers, and a tunable laser at central wavelength ~1310 nm, all on a 7.5 × 3 mm² single chip fabricated with III-V on silicon processes. The phased array is calibrated with self-evolving genetic algorithm to enable beam forming and steering in two dimensions. Distance measurement is performed with a digital signal processing that measures the time of flight (TOF) of pulsed light with a system consisting of an avalanche photodiode (APD), trans-impedance amplifier (TIA), analog-digital converter (ADC), and a processor. The LIDAR module utilizing this system can acquire point cloud images with 120 × 20 resolution with a speed of 20 frames per seconds at a distance up to 20 meters. This work presents the first demonstration of a chip-scale LIDAR solution without any moving part or bulk external light source or amplifier, making an ultra-low cost and compact LIDAR technology a reality.

Introduction

Recently a light detection and ranging (LIDAR) has emerged as significant interests in various fields, such as autonomous vehicles, robotics, and augmented-reality applications [1]. Using an optical LIDAR system brings a huge advantage over typical microwave-based radar systems as the optical wavelength affords smaller angle diffraction and enables long range and high-resolution imaging in three dimensions (3D).

LIDAR normally requires beam scanning in order to detect the surrounding environment. Most of the commercially available long-range LIDARs are based on mechanical beam scanners with rotating motors and mirrors, but they come with disadvantages such as reliability issues, large sizes, and high costs [2]. As an alternative, solid-state approach is attracting a lot of attention, because they are expected to overcome the disadvantages of mechanical counterparts. Among the solid-state approaches, silicon photonics could provide an integrated solution for the beam scanners, and the most popular form has been the optical phased arrays (OPA) that enable free-space two-dimensional (2D) beam scanning without mechanically moving parts [3-7].

The OPA exploits the same principle of phased antenna array in radio frequency (RF) technologies. Typical OPA includes a light source, cascaded splitters, phase shifters, and an array of radiating antenna. Each antenna emits coherent light with an optical phase controlled to form collectively constructive interference only in the target direction. When a phase gradient is applied to tunable phase shifters, beam scanning in azimuthal direction can be achieved. The beam scanning in the vertical direction is generally possible through wavelength tuning of the light emitted from a surface grating.

There have been several works of designing LIDAR system using OPA as a main beam scanning unit. However, most of them reported so far have used external laser sources, which critically limits the speed, size, and cost of the LIDAR systems [6]. A one-chip beam scanner with an integrated tunable laser diode (TLD) and semiconductor optical amplifiers (SOAs) on OPA chip has been reported [7], but its use in a LIDAR system has not been presented yet, presumably because of the limited optical output power.

The purpose of this project is to develop a solid-state single-chip LIDAR module based on fully-integrated optical phased arrays (OPA) to overcome the disadvantages of current LIDARs.

Method

Device Preparation

We fabricated a fully functional beam scanner on a single chip OPA of size 7.5 x 3 mm². All the optical components, such as wavelength-tunable laser (TLD), splitters, optical amplifiers, phase shifters, and grating antenna, were integrated on the chip using III-V on silicon processes, as shown in Fig. 1. The laser beam generated at the TLD is divided into 32 channels through cascaded beam splitters, and the phase shifter at each channel adjusts the 32 optical phases. The optical powers attenuated in the circuit are amplified through the 36 SOAs (4 in the 1st stage + 32 in the 2nd stage), and finally the focused optical beam is emitted from the grating-based antenna array. The TLD is typical Vernier laser composed of one SOA and two ring heaters and the wavelength can be tuned by controlling heater currents. The principle and the performance of TLD can be found in ref. [8, 9].
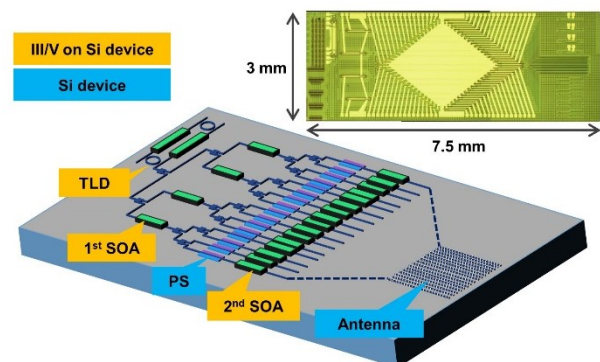

Figure 1. Illustration and microscope image of fully integrated 32-channel beam scanner. The silicon-based elements (phase shifters (PS) and grating antenna) and III/V elements (TLD and SOAs) are marked with different colors. The chip size is 7.5 mm × 3.0 mm.

Beam Steering

The two-dimensional beam scanning of OPA is achieved by adjusting the wavelength and optical phase. For the vertical beam scanning (θ) with wavelength control, a look-up table (LUT) of proper operating conditions over the ring heaters was pre-determined. Selected beam profiles for different vertical radiation angles and the corresponding cross-sectional profiles are shown in Fig. 2(a). Because the φ-direction beam shape optimization is not yet performed, the output beam is emitted as a uniform arc shape. The side-mode-suppression ratio (SMSR) was measured to be ~20 dB, which is sufficient to suppress the interference caused by the side mode.
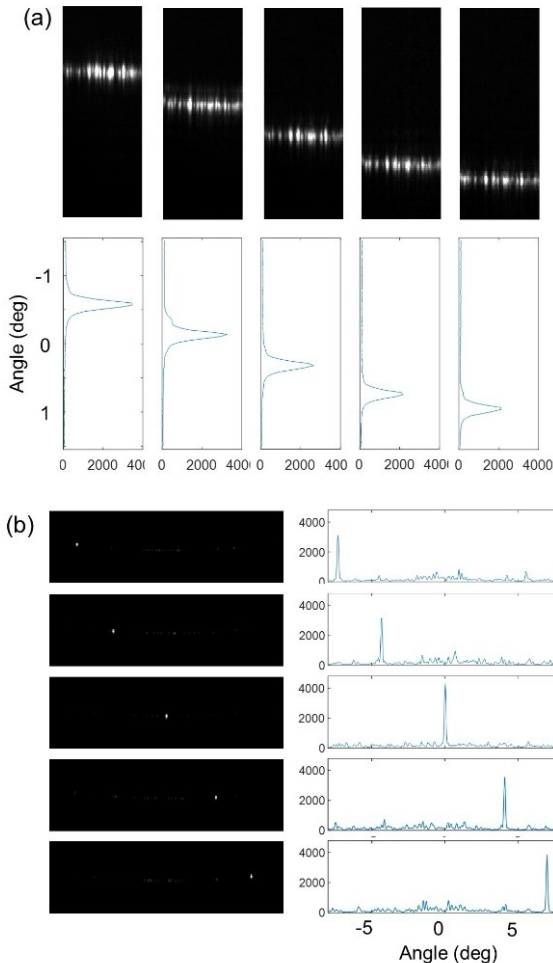

Figure 2. Beam steering demonstration by optical phased array. (a) Selected InGaAs camera images of output beam profiles from OPA and cross-section profiles during vertical beam steering by wavelength tuning. (b) Selected InGaAs camera images cross-section profiles during horizontal beam steering by optical phase tuning.

For horizontal beam scanning (φ) with phase control, another LUT with combinations of all phase shifters was needed. Ideally, the output beam can be focused towards the center when all channels in OPA are in phase. However, though the optical paths for all channels have the same travel length, the optical phases are randomized in the fabrication process. Therefore, the phase of each channel needs to be properly calibrated, but it is a very challenging

issue due to the large number of OPA channels. Here an optimization properly combining genetic algorithm and local-search approach was applied to find global solution for optical phases. Fig 2(b) shows selected beam profiles and the corresponding cross-sectional profiles at a fixed wavelength for various horizontal radiation angles in a range from -7.5 to +7.5 degrees. The SMSR measured for 120 points over the horizontal FOV was 2-10 dB, which is relatively worse compared to typical OPA cases due to the small channel count and immature processes, but still decent LIDAR operation can be achieved. The beam divergence was measured to be 0.15° × 0.09°, which is in good agreement with the design prediction.

LIDAR Module Configuration

The LIDAR module configuration is illustrated in Fig. 3. A drive board was designed to control the OPA chip, including applying voltage to TLD heaters and phase shifters for wavelength and phase control, switching on the all SOAs in TLD and waveguide channels, and generating modulation signal to run all the SOAs and phase shifters in pulsed mode. The voltage range for heaters and phase shifters were 0-8 V and 1.3-1.7 mV, respectively. The currents of all SOAs were set to 100-300 mA range and the post beam-forming optical power was measured to be ~10 mW. Pulsed mode with 30 ns width at 1 MHz was used to measure the time of flight (TOF) of light. III-V Avalanche-Photo-Diode (APD) arrays with 16 × 5 pixels were used to detect the reflected light pulses from the object and convert them to electrical signals. A two-inch diameter sized spherical lens was installed in front of the APD array. During the imaging, only 2 out of 16 columns were switched on according to the angle of the light passing through the lens and incident to the detector to minimize unwanted input such as side-lobes or other background light and dark current of remnant columns.
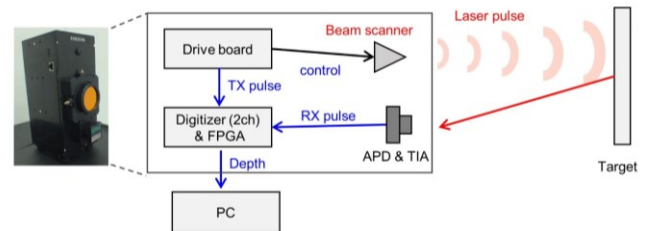

Figure 3. Illustration of OPA-LIDAR module adopting single-chip optical phased array (OPA) as a beam scanner, APD array as a detector, ADC (digitizer) and FPGA as signal processing unit. Inset photograph is LIDAR module of size 3.8 liters.

Digital Signal Processing

The distance of the target is determined by time of flight of light between transmitting signal (TX) and receiving signal (RX). The TX from the driving board and RX from the detector were transferred to analog-digital converter (ADC) circuit with a 1 GHz sampling rate. The time-of-flight (TOF) and quality of signal (QOS) were measured by calculating cross-correlation of TX and RX signals [10]. The discrete cross-correlation between TX (x) and RX (y) with signal length N is defined as following equation:

$$R_{xy}i = \sum_{k=0}^{N-1} x_k y_{i+k}\,,$$
$$i = -(N-1), -(N-2), \dots, -1, 0, 1, \dots, (N-1) \quad (1)$$

In a processor, since the calculation of cross-correlation with the above equation requires too many calculations, with order $\sim N^2$, the calculation was performed at the field programmable gate array (FPGA) by applying fast Fourier Transform (FFT) that requires $\sim N\log N$ order of calculations.
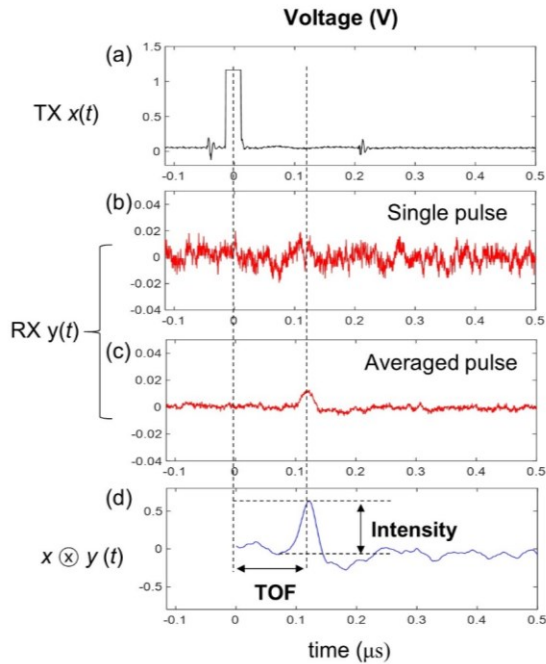

Figure 4. Digital signal processing to measure the distance of a target using cross-correlation between transmittance signal (TX, x(t)) and receiving signal (RX, y(t)). Multiple pulses are accumulated to increase the suppress white noise of detector. Time of flight (TOF) of the light and quality of signal (QOS) can be calculated from the cross-correlation between TX and RX.

Fig. 4 shows an example of digital signal processing used here. The TX signal is shown in Fig. 4(a) and the single RX signal is shown in Fig. 4(b). Before the calculation, multiple pulses are accumulated at FPGA to enhance the signal-to-noise ratio (SNR) of the RX signal, as shown in Fig. 4(c). The cross correlation result is shown in Fig. 4(d). The TOF corresponds to the delay of the TX and RX signals so that it can be measured as the maximum index of the cross-correlation, and the QOS can be measured as the maximum value of the cross correlation as an indicator for the reliability of the signal.

The measured TOFs and QOSs were collected and reconstructed in a viewer to create 3-D depth images and point clouds. The time-series data of length 1024 were collected with 1GHz rate at ADC and interpolated into 2GS/s in the processor (2048 samples in one pulse), resulting in the effective depth resolution of 7.5cm. Gathering TOFs and QOSs with 20 pulse accumulation over 120 × 20 pixels, we could achieve one depth image within 0.048 sec, leading to over 20 frames per second (FPS).

The QOS was used to filter out depth data with low reliability. Since the intensity of the reflected light is inversely proportional to the square of the range, the QOS threshold for filtering should also be determined differently depending on the distance. We measured the QOS values of the 100% reflectance object (white board) in a range of working distance and obtained a LUT for QOS threshold. Here, the QOS threshold for filtering was set to 5%, which is determined to remove noise pixels caused by white noise.

Results

Ranging Performance

The ranging performance of the LIDAR system is shown in Fig. 5. For ranging accuracy and precision analyses, averages and standard deviations of range were measured while a white flat wall was moved from 2 to 20 meters. Fig. 5(a) shows the good linearity between measured depth and ground truth with the range errors smaller than 7.5cm which is the theoretical resolution. Temporal fluctuations of depth, as shown in Fig. 5(b), was also smaller than 15 cm, or 1%, at 2 to 20 meters, indicating reliable ranging performance.
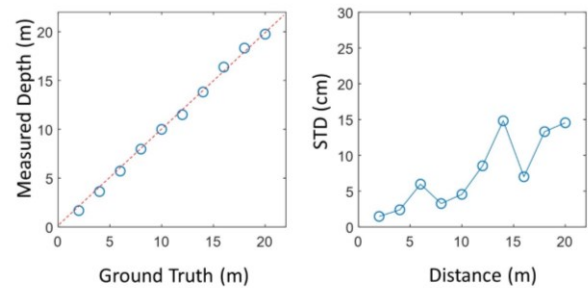

Figure 5. Evaluation of ranging performance of OPA LIDAR module. Left: Measurement of average depth value of a white wall while moving from 2 to 20 meters. Right: Measurement of temporal standard deviation of depth value of a white wall while moving from 2 to 20 meters.

Imaging Demonstration

Fig. 6 shows the sample real-time 3D depth images and point clouds obtained by the LIDAR operating 20 FPS with 120 × 20 pixels. Three white boards are located at 9 ~ 20m and a person walking around is recorded. Here we applied typical image processing techniques such as median filter, bilateral filter, flying pixel remove, and hole filling to enhance the image quality. When comparing camera images with point clouds, it is shown that the LIDAR module can accurately map the location of the objects with high spatial resolution in real time.

Conclusion

Our previous work [9] showed the LIDAR demonstration up to 10 meters with in-lab optical setup. In this work, we designed a compact solid-state LIDAR module and improved the ranging performance up to 20 meters with improved device setup, digital signal processing, and image processing. This work presents the possibility of ultra-cost and compact LIDAR technology.

However, there are still many challenges we have to address. We plan to increase the number of OPA channels for higher light output and beamforming efficiency, which will increase the
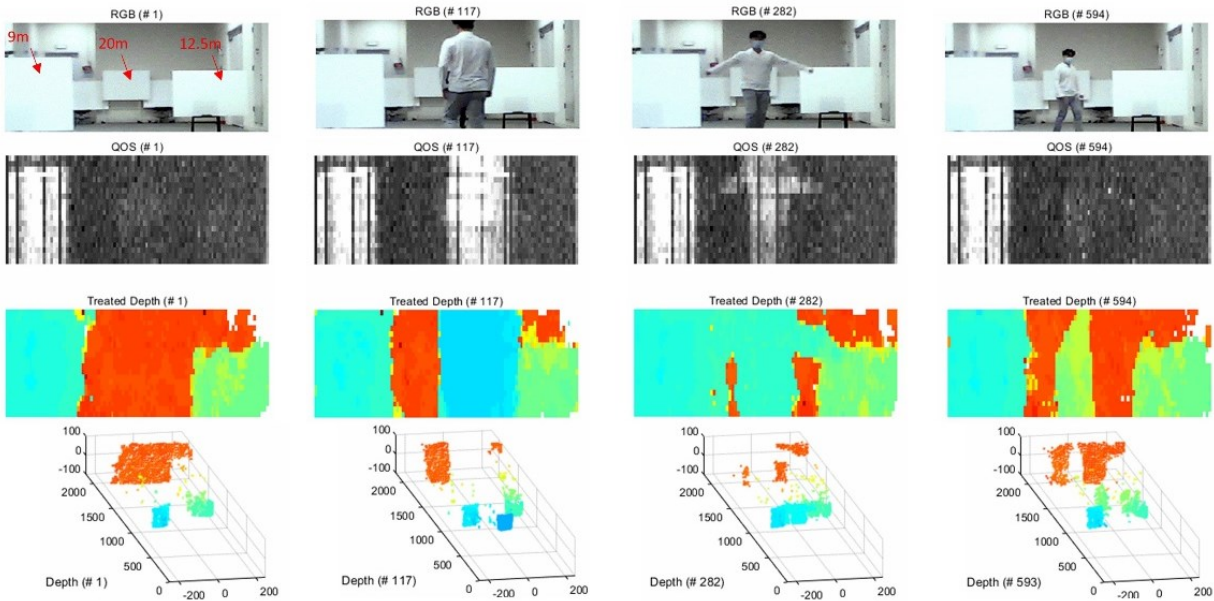
Figure 6. Real-time LIDAR demonstration at 20 FPS by a single chip beam scanner system. Camera images are shown in the 1st rose, QOS images are shown in the 2nd row, depth images are shown in the 3rd row, and 3D point cloud images are shown in the last row. The images were captured with OPA LIDAR during a person walking around three white boards located at 9, 12.5, and 20 meters. The number of pixels is 120 × 20 and the object distances are expressed with color map in depth images and point cloud images.

LIDAR's detection range and field of view. In addition, we want to increase the detection distance and image quality by improving signal processing and image processing. Finally, we are designing a small LIDAR module and are also planning imaging tests outdoors in the near future.

References

[1] Y. Li and J. Ibanez-Guzman, "Lidar for Autonomous Driving: The Principles, Challenges, and Trends for Automotive Lidar and Perception Systems," in IEEE Signal Processing Magazine, vol. 37, no. 4, pp. 50-61, 2020.

[2] I. Kim et al., "Nanophotonics for Light Detection and Ranging Technology", Nat. Nanotechnol., vol.16, pp. 508-524, 2021.

[3] J. Sun et al., "Large-Scale Nanophotonic Phased Array". Nature, vol. 493, pp. 195-199, 2013.

[4] D. N. Hutchinson et al., "High-Resolution Aliasing-Free Optical Beam Steering", Optica, vol. 3, pp. 887-890, 2016.

[5] T. Komljenovic et al., "Sparse Aperiodic Arrays for Optical Beam Forming and LIDAR", Opt. Express, vol. 25, pp. 2511-2528, 2017.

[6] C. V. Poulton et al., "Coherent Solid-State LIDAR with Silicon Photonic Optical Phased Arrays", Opt. Lett., vol. 42, pp. 4091-4094, 2017.

[7] J. C. Hulme et al., "Fully Integrated Hybrid Silicon Two Dimensional Beam Scanner", Opt. Express, vol. 23, pp. 5861-5874, 2015.

[8] D. Shin et al., "Heterogeneously Integrated Light Sources on Bulk-Silicon Platform", in 2018 IEEE International Electron Devices Meeting (IEDM), pp. 23-6, 2018.

[9] J. Lee et al., "Single-Chip Beam Scanner with Integrated Light Source for Real-Time Light Detection and Ranging," in 2020 IEEE International Electron Devices Meeting (IEDM), pp. 7.2.1-7.2.4, 2020.

[10] J. Lee & J. Kim, "Lidar Device and Operating Method Thereof", U.S. Patent Application no. 16/782779, 2019.

Author Biography

Jisan Lee received his BS and PhD in material science and engineering from Pohang University of Science and Technology (POSTECH) in 2009 and 2014. Since 2015, he has worked in Samsung Advanced Institute of Technology in Samsung Electronics. He is currently working on developing LIDAR based on silicon photonics, mainly focusing on sensor control, calibration, and signal processing